Conf-9404100--4

LA-UR- 94-1813

Title: FREE-FIELD GROUND MOTIONS FOR THE NONPROLIFERATIO EXPERIMENTS PRELIMINARY COMPARISONS WITH NEARBY NUCLEAR EVENTS

Author(s): Anthony L. Peratt, P-15
Kenneth H. Olsen, P-15

Submitted to: DOE Symposium on the Nonproliferation Experiment Result and Implication for Test Ban Treaties

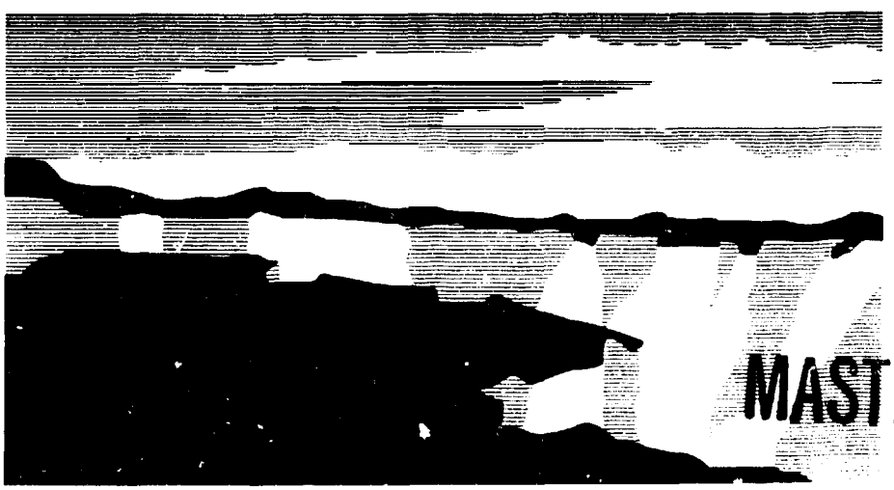

Los Alamos
NATIONAL LABORATORY

FREE-FIELD GROUND MOTIONS FOR THE NONPROLIFERATION EXPERIMENT: PRELIMINARY COMPARISONS WITH NEARBY NUCLEAR EVENTS

KENNETH H. OLSEN and ANTHONY L. PERATT

Explosion Effects Physics Project, Group P-15, Los Alamos National Laboratory, Los Alamos, NM 87545, **kolsen@geophys.washington.edu; alp@aerie.lanl.gov.**

Revised Abstract

Since 1987, in an effort to provide more extensive ***close-in (<10 km) data*** **sets** for modem regional and teleseismic source function studies, we have installed fixed **arrays** of **tri-axial** accelerometers in the free-field near the shot horizons for low-yield (≤ 20 kt) nuclear events in the N-tunnel complex beneath Rainier Mesa. For the Nonproliferation Experiment **(NPE)** we augmented the array to achieve 23 **free-field** stations. Our accelerometer arrays span distance intervals between the non-linear material failure **region**—where peak **stresses** are the same order as rock strengths **(<200** bars and ranges typically **~50–150 m)—and** distances (-1 km) where linear-elastic response is expected (stress **<50** bars; accelerations **<1 g).** Goals are: (a) to examine robustness and stability of various free-field source function **estimates**—***e.g.***, reduced displacement potentials **(RDP)** and **spectra; (b)** to compare close-in with regional estimates to test whether detailed close-in free-field and/or surface ground motion data can improve predictability of regional-teleseismic source functions; (c) to provide experimental data for checking two-dimensional numerical simulations. We report preliminary comparisons between experimental free-field data for NPE (1993) and three nearby nuclear events (MISTY ECHO, 1988; MINERAL QUARRY, 1990; HUNTERS TROPHY, 1992). All four working points **are** within 1 km of each other in the same wet tuff bed, thus reducing concerns about possible large differences in material properties between widely separated shots. Initial comparison of acceleration and velocity seismograms for the four events **reveals**: (1) There is a large departure from the spherical symmetry commonly assumed in analytic treatments of source theory; both vertical and tangential components are surprisingly large. (2) All shots show similar first-peak particle-velocity amplitude decay rates $\sim R^{-1.8}$ suggesting significant attenuation even in the supposedly purely elastic region. (3) ***Sharp*** **(>20** Hz) arrivals are ***not*** observed at tunnel level from near-surface **pP** reflections or **spall-closure** sources---but broadened peaks are seen that suggest more diffuse reflected energy from the surface and from the Paleozoic limestone basement below tunnel level.

Introduction

Close-in free-field measurements of stress wave propagation in geologic media with well-documented material properties can play a unique role in establishing a fundamental physical basis for predicting equivalent elastic seismic source functions for most types of underground explosions in arbitrary geological environments. Since 1987, as part of a coordinated experimental program to study the basic physics of the evolution of explosion waves from the hydrodynamic and highly non-linear material response regions very close to the source out to purely elastic motions at distances c 10 km, we installed fixed arrays of tri-axial accelerometers in the free-field at the shot horizons for low-yield (I 20 kt) nuclear events in N-tunnel complex beneath Rainier Mesa at NTS. We supplemented the arrays for additional free-field observations of the Non-Proliferation Experiment (NPE). Our main purpose has been to help bridge the "knowledge gap" between numerous essentially high-pressure equation of state (EOS) and shock physics studies very close to the explosion and the also numerous surface seismic measurements made at distances beyond a few km. Our measurements focus principally on the "nonlinear-to-linear transition zone" at distances between about 50 m and 1000 m, which should include the indistinct region loosely known as the "elastic radius.*' Goals are both (a) to provide experimental "ground-truth" data for detailed comparison with state-of-the-art two-dimensional numerical models, and (b) to provide detailed free-field data in the vicinity of the "elastic radius" against which seismic inversion and equivalent source function scaling techniques can be critically tested.

Table 1 is a summary of locations and seismic parameters for the four underground explosions at N-tunnel for which we have made free-field observations. In a previous paper (Olsen and Peratt, 1993), we made selected comparisons of *first peak (only) transient values* of acceleration, particle velocity, and displacement for the three nearby nuclear events (MISTY ECHO, 1988; MINERAL QUARRY, 1990; HUNTERS TROPHY, 1992) preceding the NPE. In this short contribution, we show preliminary free-field results from our NPE observations together with selected data from the MISTY ECHO nuclear event, but we will present *waveform data* in preference to only transient first-peak values. However, because the yields of the nuclear shots have not yet been declassified, we are unable at this time to present a satisfactory detailed quantitative comparison between the nuclear and "chemical" sources. Instead, we will stress general features of the waveform data for all four explosions that pertain chiefly to the basic physical processes occurring in the free-field, nonlinear-to-linear transition zone. More extensive analyses using spectral and reduced displacement (RDP) techniques are underway but will not be reported here.

Free-field waveform data

Figure 1 is a schematic cross section showing general features of underground free-field accelerometer array installation for our Rainier Mesa seismic source physics experiments. Figure 2 displays a plan view of part of the N-tunnel complex and shows the final 23-station configuration of the accelerometer array that was in place for the NPE. As discussed in the caption, the N-tunnel accelerometer array grew piecemeal with time as successive shots were planned and executed over the years in the N-tunnel complex; only seven stations were installed for the initial 1988 MISTY ECHO shot, for instance. In designing the underground arrays, we always tried to achieve as broad range-interval and azimuthal distributions with respect to each new source as was possible within the tunnel-access constraints of the time. Because most of our instrument packages operated by design in the distal portions of the crush and shear region where peak accelerations and stresses seldom exceeded ~500 g and -1 kilobars respectively, most of these grouted, sealed instrument packages with associated cabling usually survived and could be reactivated for succeeding shots. However, this often meant that individual instrument sensitivities (i.e., Volts/g) and gauge linearity limits (both unchangeable after initial grouting-in) could not be optimized for following experiments. In practice, as the number of stations in the array grew, most new added instruments were high-g-limit units installed close to the newest working point in order to acquire as much new data in the nonlinear material (rock) response regime as possible.

For several reasons, the 7-station MISTY ECHO (ME) array achieved the highest performance of all of the 4 experiments in terms of gage sensitivity, fully optimized digital dynamic recording ranges, and lowest electrical and data processing noise levels. The MISTY ECHO data set thus usually displays the clearest examples of many of the general free-field waveform characteristics that we wish to point out in this contribution. We will first overview the NPE data and then display selected waveform plots from the ME data set in order to better understand the more important general characteristics of the free-field data sets from all our N-tunnel experiments.

(A word of caution in viewing the plots is in order: We display here mainly *velocity* and *displacement* waveforms which are derived by integration of the primary ***acceleration data.*** After integration, one normally makes corrections (1) for long-term trends aue to any electronic noise introduced by the data processing/recording system hardware and also (2) to remove 'ramps,' and trends resulting from the integration process. For example, integrated *velocity* values should return to the zero baseline at very long times (> 20 s in our case). However, our initial attempts to apply very simple filtering and correction processes to achieve this often severely modified 'intermediate' frequency (-1-2 Hz) signals that were obviously geophysical in origin. For this initial overview, we have elected *not* to apply any long-term corrections. Thus, values for some

integrated parameters, such as "permanent" particle displacements, steady-state values of the RDP, and "'DC-levels" for spectra should be recognized as possibly somewhat uncertain and inaccurate at this time.)

Slant-range and gauge performance data for the NPE free-field array is summarized in Table 2. Unfortunately, due to a faulty grout mixture during installation of the four new high-g units (TM 31-34) closest to the NPE charge about 10 months prior to the shot, these gauges failed at very low stress levels and gave invalid acceleration readings shortly after initial shock arrival. Thus, much of the higher-stress-EOS portion of our experiment was lost, but most of the more distant existing stations yielded good data that extended well into the elastic zone.

Figures 3a, 3b, and 3c display the first two seconds of the NPE *particle* velocity records for the Radial, Tangential, and Vertical (Z) components respectively. ***A priori,*** one would expect to observe that the higher Frequency energy is attenuated more rapidly with distance due especially to nonlinear crush and shear processes close-in. Indeed, this initial pulse broadening and selective attenuation of higher frequencies in the coda during about the first second of record can be seen—particularly on the radial and vertical components. (This effect is displayed even more clearly on the ME records of Fig. 6a and Fig. 6b).

While one can readily trace the evolution with distance of several high-frequency waveform features and phases on both the radial- and vertical-component stacks, transverse-components (Fig. 3b) appear to show very little coherence in this respect between successive seismograms in the stack. Indeed, there appears to be poor consistency even in the polarities of the initial pulses. We interpret this to mean that transverse energy arises here mainly from scattering and multi-pathing due to small, random inhomogeneities throughout the bedded tuffs of Rainier Mesa. We intend to evaluate such effects more thoroughly by future detailed studies of both acceleration and velocity spectra.

The NPE vertical component velocity waveform stack (Fig. 3c) displays many of the same high-frequency (~50 Hz) features and phases shown on the corresponding radial seismograms (Fig. 3a). There is a high coherence between the radial and vertical seismograms (high R-Z coherence also is seen on the primary accelerograms). The good coherence between radial and vertical components for N-tunnel free-field data is principally due to the fact that there is a particular bedded tuff layer immediately below tunnel level in this part of Rainier Mesa which has a strong positive velocity gradient (velocity increases downward). Thus, much initially down-going energy is refracted back upward by this strong positive gradient; significant vertically-traveling energy is evident on all our seismograms—even at the closest ranges ~50 m. Also of great interest are the

"long-period" (~ 2 Hz) oscillations that are particularly evident on all the vertical velocity-seismograms. These oscillations can also be seen, but less obviously, on the radial component waveforms, but appear only intermittently and less clearly on transverse components. Similar long period oscillations-chiefly on the vertical components-appear on free-field seismograms for all four N-tunnel shots, both for the NPE ANFO charge and for all three nuclear sources. These long-period oscillations are most clearly seen on the MISTY ECHO vertical velocity records (Fig. 6b). We will comment more extensively on these oscillations when we discuss details of the ME records below.

Figure 4 displays Radial, Transverse and vertical component velocity waveforms for a single triaxial NPE station (TM- 10), all plotted at the same amplitude and time scales. One is immediately struck with how large are the m-is-amplitudes (particularly for frequencies >10 Hz) of the vertical and transverse components as compared with corresponding radial component amplitudes. We clearly observe this near-equality of rms component-amplitudes on almost every station for all four shots (e.g., see also the ME station discussed in Fig. 7 below). Thus, there obviously is a very large departure from the spherical symmetry that commonly is assumed in analytic treatments of source theory. This suggests that one should carefully re-evaluate the practice of comparing only radial-component, close-in, free-field data with spherically-symmetric equivalent seismic source functions &rived from inversion of distant seismic observations. We noted above that the relatively large amplitudes of vertical components has at least a partial explanation because of strong upward refraction from the strong velocity gradient just beneath tunnel level, but this cannot satisfactorily account for all the effect in the surprisingly large transverse components. In discussing transverse waveforms in Figure 3b, we suggested that much of the non-radial, higher-frequency energy arises from scattering and multi-path propagation due to roughly meter-size inhomogeneities of the surrounding geological medium. Strong scattering and multi-pathing would lead to an effective equipartitioning of rms energy over propagation distances of a few tens- to hundreds-of-meters. In all our tunnel experiments, we do indeed observe (&tails not shown here) such an increase in equipartitioning versus propagation distance both with respect to rms amplitudes and for first-peak transient acceleration, velocity, and displacement pulses. In previous surface-array ground motion measurements on shots in the alluvium of Yucca Flats (Stump, et al., 1994), we have also seen strong evidence in displacement spectra for long-duration, complex wave trains and equipartitioning between components. In the Yucca Flats alluvium experiments, however, the distance-scale over which the equipartition process takes place appears to be about ten-times greater than that for tunnel tuffs (i.e., for alluvium, waveforms/spectra are 'simple' at ranges -500 m but complex/'equipartitioned' at -5 km, whereas for N-tunnel tuffs the corresponding distances are more like 50 m and 500 m, respectively.

The other noteworthy feature seen in Figure 4 (and already pointed out in comments on Fig. 3c above) is the "2-Hz long-period" oscillation which is particularly well developed on the vertical component at times after 0.5 s. In Figure 4, we observe that this "2-Hz" oscillation also is seen quite well on the radial component and is effectively in phase with the vertical oscillation. However, the case for a corresponding long-period oscillation on the transverse component is unconvincing. Again, we defer discussion of the long period oscillation until we examine some MISTY ECHO records below.

We now tum to an examination of selected MISTY ECHO waveforms. As noted above, the reason for discussing ME records here is that most general characteristics of all our the free-field data sets are particularly well displayed due the more optimal recording conditions for the ME shot. Figure 5 shows the evolution with distance of the radial component displacement (doubly integrated acceleration) waveforms for ME. These nicely illustrate "overshoot*' and "rebound" of transient free-field displacements and the eventual decay to a "permanent" displacement value. For instance, at the closest ME station (TM-2 at 341-m-range) the displacement of the tuff medium first expands to about 25 cm (overshoot), then rebounds back to 7 cm and then expands again to reach an apparent steady- state value of about 12 cm after 2 seconds. These motions mirror similar but larger motions of the explosion cavity wall. Although not shown here, vertical and transverse components of displacement show similar waveform characteristics, but again, these amplitudes are surprisingly large. (Comfortingly, "permanent" displacement values for both T- and Z-components in these uncorrected ME records return to within a few millimeters of zero.) We note that the full sequence of overshoot-rebound-steady-state takes place in a time scale of about 2 seconds. This implies that good free-field records of at *least* two-seconds-duration are required in order to derive reliable estimates for ***long-period*** RDP parameters for NTS tunnel shots. (We maintain that good records of at least 10-s duration are necessary to &rive meaningful estimates of long-period spectral levels [for moment estimation].)

We return to examining velocity waveforms in the remaining figures. Figures 6a and 6b display the evolution with distance of MISTY ECHO velocity waveforms for radial and vertical components, respectively. Due to the much lower long-term drifts in the ME data as compared to NPE, it is possible to display 5-second-duration records in Figures 6a and 6b rather than only 2 seconds as for NPE (Figs. 3a, 3b, and 3c). Comparing radial components for the two events (Fig. 6a and Fig. 3a), we again note the broadening of the initial pulse and the selective decay of higher (>20 Hz) frequencies in the pulse coda, probably mainly due to strong, close-in attenuation processes-including non-linear crush and shear particularly at ranges <200 m. Although we are unable to quantitatively demonstrate them here because of classification constraints, comparison of

initial peak values **of acceleration (directly related to peak forces** on buried structures), velocity, and displacements for the three nuclear sources versus those from the NPE ANFO charge suggests the lower-energydensity NPE event is about ***twice as effective*** as ***tamped nuclear sources as*** **in producing mechanical effects, such as peak shock forces on buried structures, etc.** Such an approximately double equivalency factor for completely buried High-Explosive charges ("TNT") over tamped nuclear sources has been well known for a number of years among nuclear effects modeling and explosion **cratering** specialists within the U.S. defense research community (e.g., **Killian,** et al. 1987). Although the approximate HE/nuclear equivalency factor quoted here refers strictly to the **stronger** high-frequency signals near the beginning of the **free-field** waveforms, our **preliminary** evidence suggests that a nearly equal factor also pertains to the lower-frequency energy characterizing radiated seismic energy from the two source types.

Figure 6b displays vertical velocity waveforms for ME which show even more clearly several features **already** noted for NPE (Fig. **3c).** In addition, we call particular attention to the large, **"long-period"** (- 1 Hz) oscillations, in-phase on all components, which dominate the **vertical** wave trains at times **>1** S-2 seconds. We observe such 1 **-Hz** vertical oscillations at later times on all four N-tunnel shots (NPE and 3 nuclear) for which we have made free-field measurements (the **2-**secondduration NPR records of Fig. 3c arc not quite long enough to display these **clearly).** This universality leads us to tentatively conclude that these l-Hz vertical oscillations are more indicative of larger features of Rainier Mesa geological structure than they are of wave propagation effects close to the individual shot points. Consideration of an additional separate line of evidence leads us to suggest an explanation for several features of the vertical free-field seismograms. One cannot readily discern on vertical seismograms any sharp pulse returning after near-total reflections (a **pP** reflection) from the Mesa-top free-surface. Actually, there should be ***two*** reflection pulses: one due to **pP** from the surface and another from the large velocity contrast between the mesa tuffs and the Paleozoic limestone basement about 200-400 m below the tunnel-level gauges (the reflection coefficient here should be fairly large because the P-velocity contrast probably exceeds **1 km/s).** Examination of Figure 6b suggests the presence of ***two, broadened*** upward peaks at about 250 ms and **400-500** ms after the initial sharp, "shock" **pulse** on all seismograms. Pending detailed forward **modeling,** we suggest these are the diffused reflections from the free-surface above **(pP),** and from the Paleozoic limestone basement below. Thus, considerable mainly vertically-traveling, seismic energy is reflected back and forth between these two strong largely-horizontal reflectors leading to "trapping" of energy and rather coherent, mostly **vertical** oscillations which probably cause Rainier Mesa to vibrate vertically essentially as a unit. This preliminary explanation needs to be tested by more detailed data analysis and by numerical modeling.

Finally, shown in Figure 7 are radial, transverse and verticalcomponent velocity waveforms for a single triaxial MISTY ECHO station (TM-3), all plotted at the same amplitude and time scales (compare with NPE in Fig. 4). In contrast to NPE signals of Figure 4, this ME station is located at a somewhat larger peak stress level (probably still within the nonlinear crush and shear failure zone) so the radial component dominates and "equipartitioning" between components has not proceeded as far. Nevertheless, there already is significant higher frequency enn gy (> 20 Hz) in both the vertical and transverse components.

Concluding remarks

The main important points from this initial overview of the NPE free-field experiments are:

- Both nuclear & NPE shots show an approximately bi-modal energy distribution with frequency :
  1. High Frequencies (> 10-20 Hz) arise! from the expanding/attenuating shock front.
  2. Low frequency (-1-2 Hz) of lower amplitudes at later times in seismogram (Significant as a large portion of total energy radiated as seismic waves to regional and teleseismic distances).
- Conversion to low frequencies appears very efficient on vertical component seismograms (large surface [pP] and basement reflections)
- For high-frequency, first-peak strong-motion accelerations & velocities, NPE is more! efficient (roughly x 2) than tamped nuclear sources.

In surveying free-field ground motions from all four N-tunnel shots, we continue to be impressed by the large amount of close-in seismic energy residing in the vertical and transverse components and at the "non-spherical" complexity of close-in free-field ground motions even at the relatively close ranges explored by our N-tunnel experiments. This complexity suggests that considerable care needs to be observed in comparing and understanding the basic physics of seismic source function estimates as derived by close-in and oy distant seismic techniques.

References

Killian, B. G., J. R. Rocco, and E. J. Rinehart, ***Comparisons of Nuclear-TNT Equivalencies ad Effects Environments in Different Geological Media,*** Defense! Nuclear Agency, Washington, DC, ***DNA-TR-87-152, 1987.***

Olsen, K. H., and A. L. Peratt, Free-field ground motion measurements in the nonlinear-to-elastic transition region, in S. R. Taylor and J. R. Kamm (eds.), ***Proceedings of the Numerical***

Modeling for Underground Nuclear Test Monitoring Symposium, Los Alamos report LA-UR-93-3839, pp. 397-404, 1993.

Stump, B. W., R. E. Reinke, K. H. Olsen, and L. R. Johnson, Isotropic and deviatoric characterization of the Coalora nuclear explosion in Yucca Flats, *Geophys. J. Int. 116*, 538-552, 1994.

==========

TABLES

Table 1 Seismic Parameters of Four Underground Explosions in N-Tunnel, Rainier Mesa, Nevada Test Site

Table 2 Slant-ranges and gauge performance for NPE free-field array

Seismic Parameters of Four Underground Explosions in N-Tunnel, Rainier Mesa, Nevada Test Site

Event	Location				Origin Time		Magnitudes				
Event Name, Hole ID	**N Latitude**	**W Longitude**	**Surface Elevation m**	**DOE m**	Date	Time, UT (DOE)	mb (NEIC)	mb (ISC)	m_{bPn} †	m_{bLg} ‡	M_L (BRK)
MISTY ECHO U12N.23	37° 11' 56.54"	116° 12' 34.00"	2259	400	10 Dec. 1988	2030:00.055	5.0	5.0	4.81	5.16	5.0
MINERAL QUARRY **U12N.22**	37° 12' 24.73"	116° 12' 51.33"	2243	400	25 July 1990	1500:00.057	4.7	4.8	4.53	4.94	
HUNTERS TROPHY **U12N.24**	37° 12' 24.93"	116° 12' 35.94"	2239	385	18 Sept. 1992	1700:00.008	4.4		4.18*	4.57*	
NPE = (NON-PROLIFERATION EXPERIMENT) U12N.25 (a.k.a. 'CHEMICAL KILOTON")	37° 12' 06.95"	116° 12' 35.50"	2243	390	22 Sept. 1993	0701:00.080	4.1		4.16	4.59	

† For definition and discussion of the LLNL 4-broadband-station regional magnitude, m_{bPn}, see: Denny, M. D., S. R. Taylor, and E. S. Vergino, Investigation of mb and MS formulas for the Western United States and their impact on the M_S/m_b discriminant, *BSSA 77*, 987-995, 1987.

‡ For definition and discussion of the LLNL 4-broadband-station regional magnitude, m_{bLg}, see: Patton, H. J., Application of Nuttli's method to estimate yield of Nevada Test Site explosions recorded on Lawrence Livermore National Laboratory's digital seismic system, *BSSA 78*, 1759-1772, 1988.

* These are 3-station values rather than 4-station averages.

TABLE 2		
FREE-FIELD RANGES FOR NPE		
U12N.25		
Sta ID	Slant range (m)	Comments
TM 31 (L1)	54.206	Shorted @ D-2 (Grout failure)
TM 32 (L2)	84.629	Grout failure(>50g)-shock rise only (t<50 ms)
TM 6	93.987	Exceeded gauge linearity (>25g)
TM 33 (L3)	98.326	Grout failure(>50g)-shock rise only (t<50 ms)
TM 2	100.321	Exceeded gauge linearity (>25g)
TM 34 (L4)	114.226	Grout failure(>50g)-shock rise only (tc50 ms)
TM 7	228.435	Early data only-some axes failed t~1s
TM 5	384.151	
TM 9	392.315	
TM 26	406.446	
TM 8	438.789	
TM 25	450.748	
TM 13	459.779	
TM 4	472.709	Inoperative after previous shot
TM 24	475.036	
TM 14	503.870	
TM 23	504.299	
TM 1	512.146	
TM 22	514.983	Early data only-some axes failed t ~200 ms
TM 21	523.020	Inoperative after previous shot
TM 3	673.779	Inoperative after previous shot
TM 10	675.821	
TM 12	724.065	
TM 15	1099.229	

Figure Captions

Fig. 1. Cartoon cross-section of Rainier Mesa, NTS, illustrating the general layout of triaxial free-field accelerometer units in relation to the close-in, high-stress gauges and the mesa-top surface measurements fielded by other experimenters. Oriented triaxial free-field accelerometer packages are typically grouted into boreholes at depths at least 2-tunnel-diameters (6 m) below the tunnel floor in or&r to eliminate small effects of tunnel-wall motions on the desired free-field accelerograms.

Fig. 2. Map of part of the N-tunnel complex (approximately 400 m beneath the mesa surface) showing locations for the 23-station free-field accelerometer array activated for the Non-proliferation experiment (NPE). Also shown are the working points (★) for three previous nearby nuclear events (MISTY ECHO [ME]; MINERAL QUARRY, [MQ]; and HUNTERS TROPHY [HT]) which were recorded by fewer-station predecessors of our free-field accelerometer network. [The first event, ME, had only a seven stations (#'s: 2, a pair near 4, 6, 7, 8, and 12). Stations 1, 3, 5, 9, 10, 14, and 15 were added for MQ; stations 21-26 were added for HT; and stations 3 l-34 were added for NPE.] Depending somewhat on source yield, stations generally closer than about 100-200 m from the WP undergo non-linear material failure (crush and shear), whereas beyond 200-300 m, rock responses are nearly elastic.

Fig. 3a. Stack of trace-normalized particle-velocity seismograms from the NPE arranged in or&r of distance (see Table 2) from the NPE working point. (a) Radial components. (b) Tangential components. (c) Vertical components. Only the first 2 seconds of the seismograms are shown. Note how the first transient pulse broadens and the dominant frequencies of the first 1 second of high-frequency (-50 Hz) coda decrease with range. Also, observe the approximately 2-Hz low-frequency, in-phase energy appearing mainly on vertical components (Fig. 3c). No corrections have been made for any offsets or long-period drifts arising from either the recording system or from integration of primary acceleration data.

Fig. 3b. Tangential components. (See caption for Figure 3a)

Fig. 3c. Vertical components. (See caption for Figure 3a)

Fig. 4 Comparison of Radial (R), Transverse (T), and Vertical (Z) component velocity waveforms from free-field station TM-10 for the NPE. Station is at a range of 676 m from the charge center, well outside the "transition zone" in a region where the tuff response should be elastic. All components are plotted at the same amplitude scale. Note that for frequencies greater

there is an approximate 'equipartitioning' of energy among all components. "Long-period" (-2 Hz) energy is clearly seen on both Z and R components. (All uncorrected for offsets or long-period drifts.)

Fig. Plot of Radial component, ***Displacement*** waveforms as function of range for the MISTY ECHO nuclear event, to illustrate 'overshoot" and "rebound'* of transient free-field displacements and the eventual decay to a "permanent*' displacement value. Because of uncertainties due to possible as-yet-uncorrected long-term instrumental and integration drifts, some caution about the precision of 'permanent' displacement values is recommended. (Trace-normalization; no corrections for offsets or long-period drifts.)

Fig. 6a volution of the Radial-component, ***Velocity*** waveforms for the MISTY ECHO event. Compare with (It-second) NPE data shown in Figure 3a. Again, note loss of high frequencies in initial pulse coda for greater distances. (Trace-normalization; no corrections for offsets or long-period drifts.)

Fig. 6b volution of the Vertical-component. ***Velocity*** waveforms for the MISTY ECHO event. Compare with (2-second-duration) NPE data shown in Figure 3c. Particularly note the two broadened upward peaks (arrows) at about 250 ms and 400-500 ms after the first, sharp, "shock" pulse on all seismograms. Pending detailed forward modeling, we suggest these are diffused reflections from the free-surface above (pP), and from the Paleozoic limestone basement about 200-400 m below these tunnel-level gauges. As for radial components, the loss of high frequencies in the initial pulse coda at greater distances is evident. Also noteworthy are the "long-period," in-phase oscillations which here show frequencies somewhat below 1 Hz for times greater than 2 seconds. (Trace-normalization; no corrections for offsets or long-period drifts.)

Fig. 7 Comparison of Radial (R), Transverse (T), and Vertical (Z) component, ***velocity*** waveforms from free-field station TM-3 for the MISTY ECHO nuclear shot. Station is at a range of 492 m, which-for the somewhat larger yield ME event-places it in the outer portion of the non-linear ("crush and shear") transition zone. Compare with NPE data of Figure 4. Again, the approximate 'equipartitioning' of energy among components is noticeable even at this position somewhat inside the "elastic radius" for this shot.

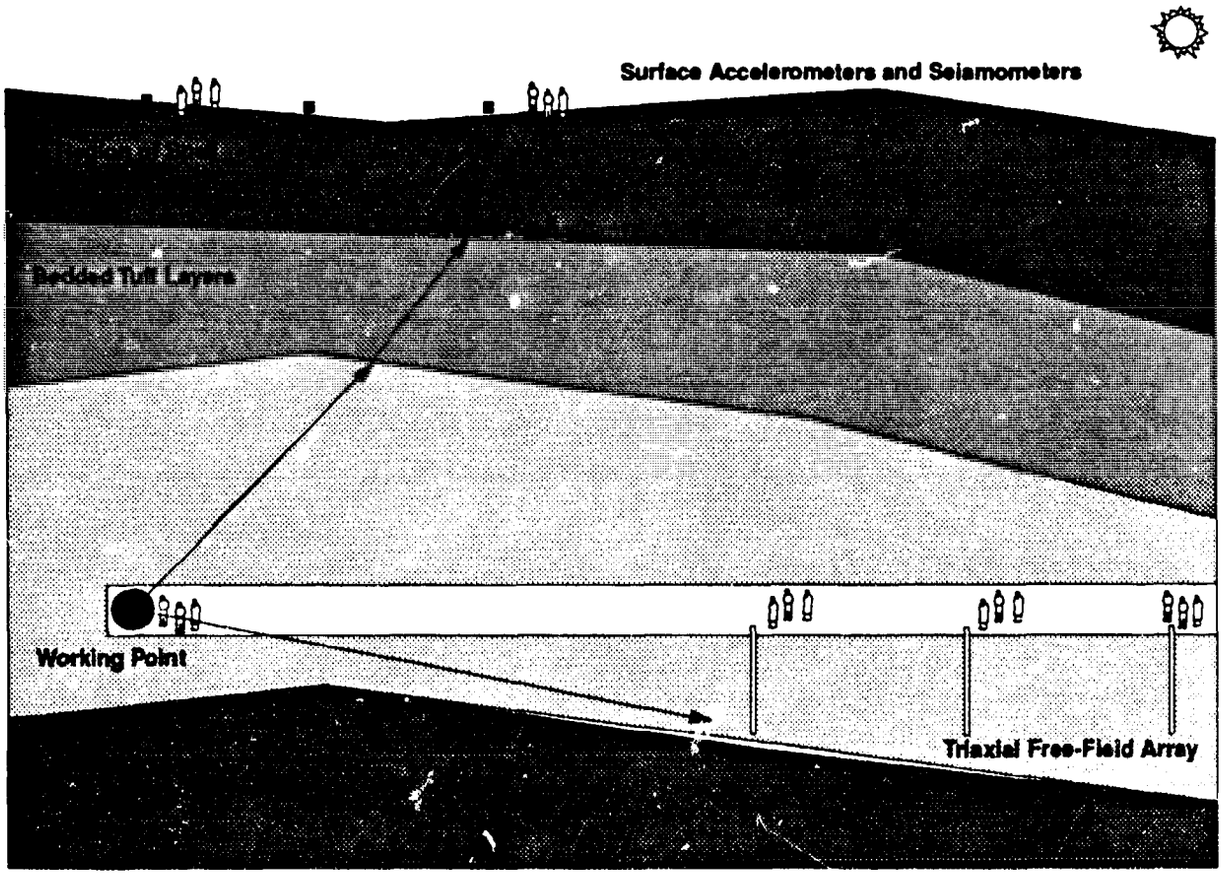
Surface Accelerometers and Seismometers
Working Point
Triaxial Free-Field Array

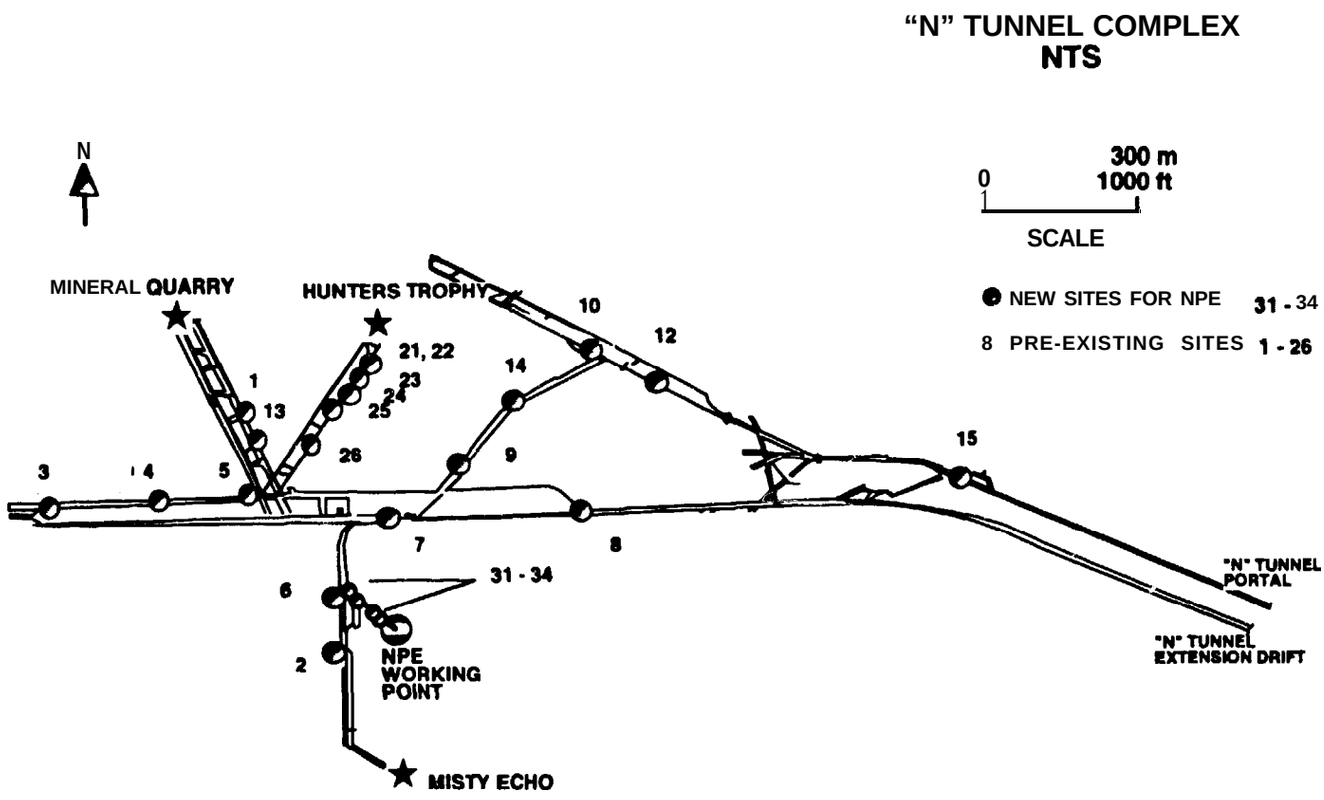

Free-field accelerometer array for the Non-Proliferation Experiment

NPE Velocities - Radial

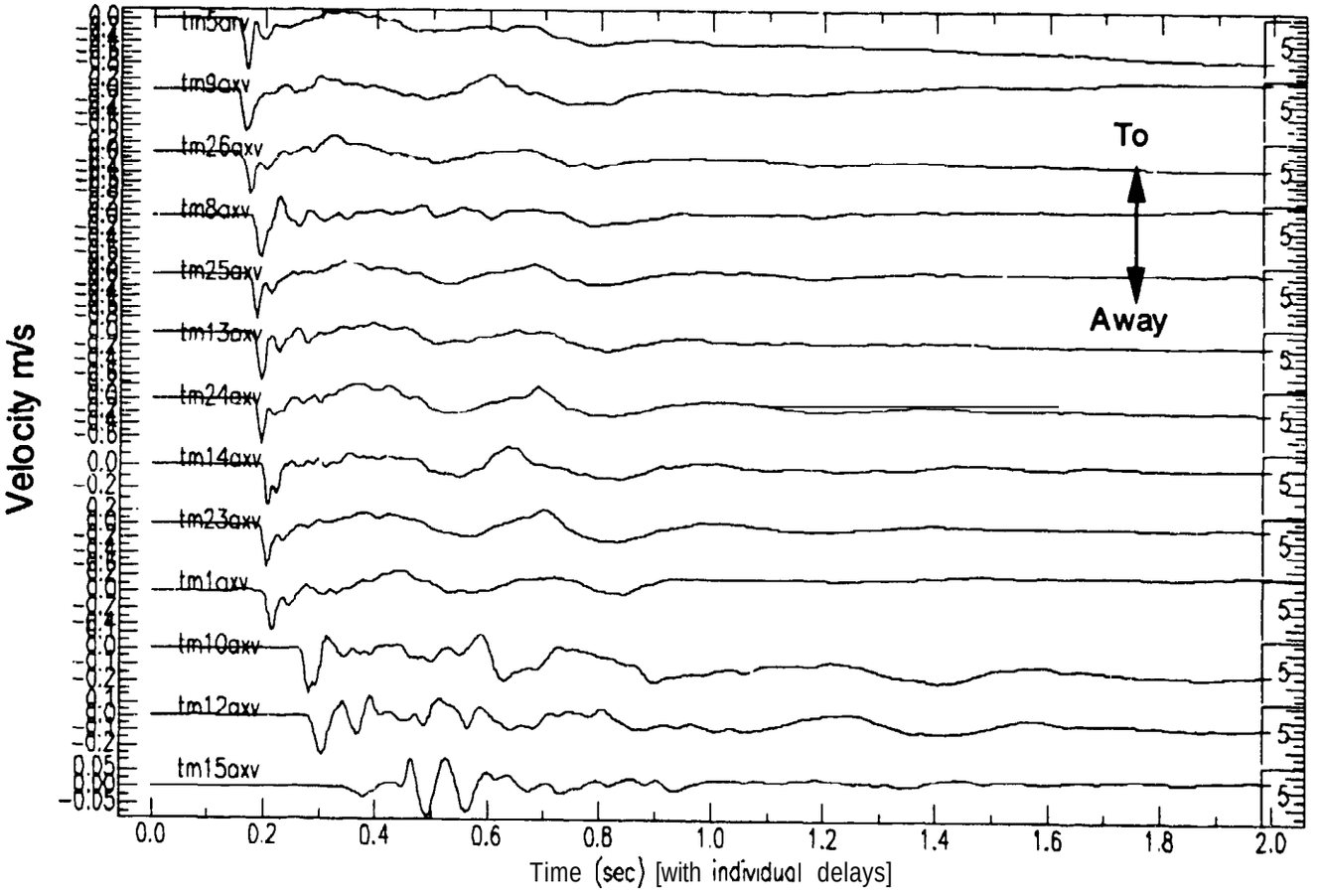

NPE Velocities - Transverse

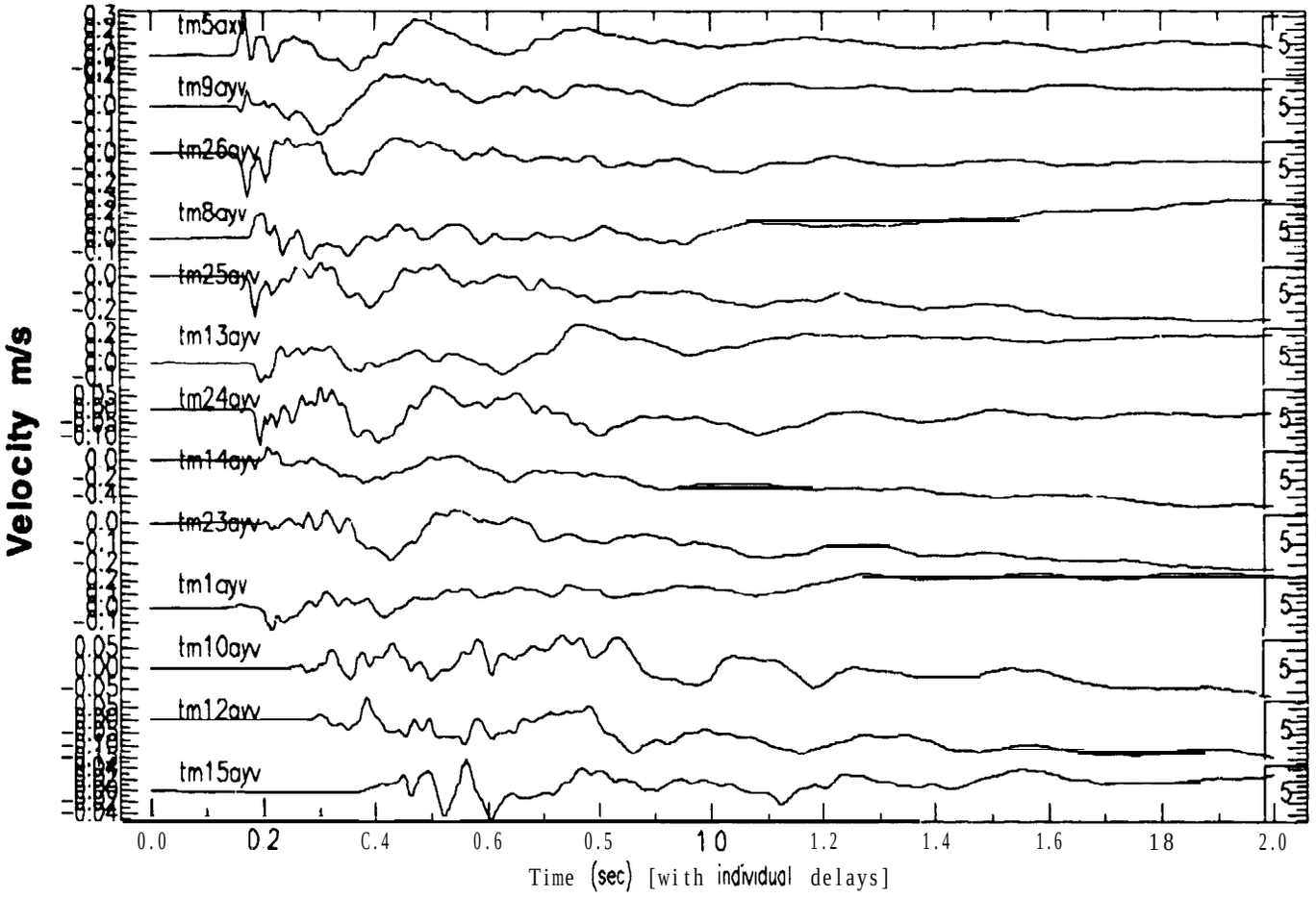

NPE Velocities - Vertical (Z)

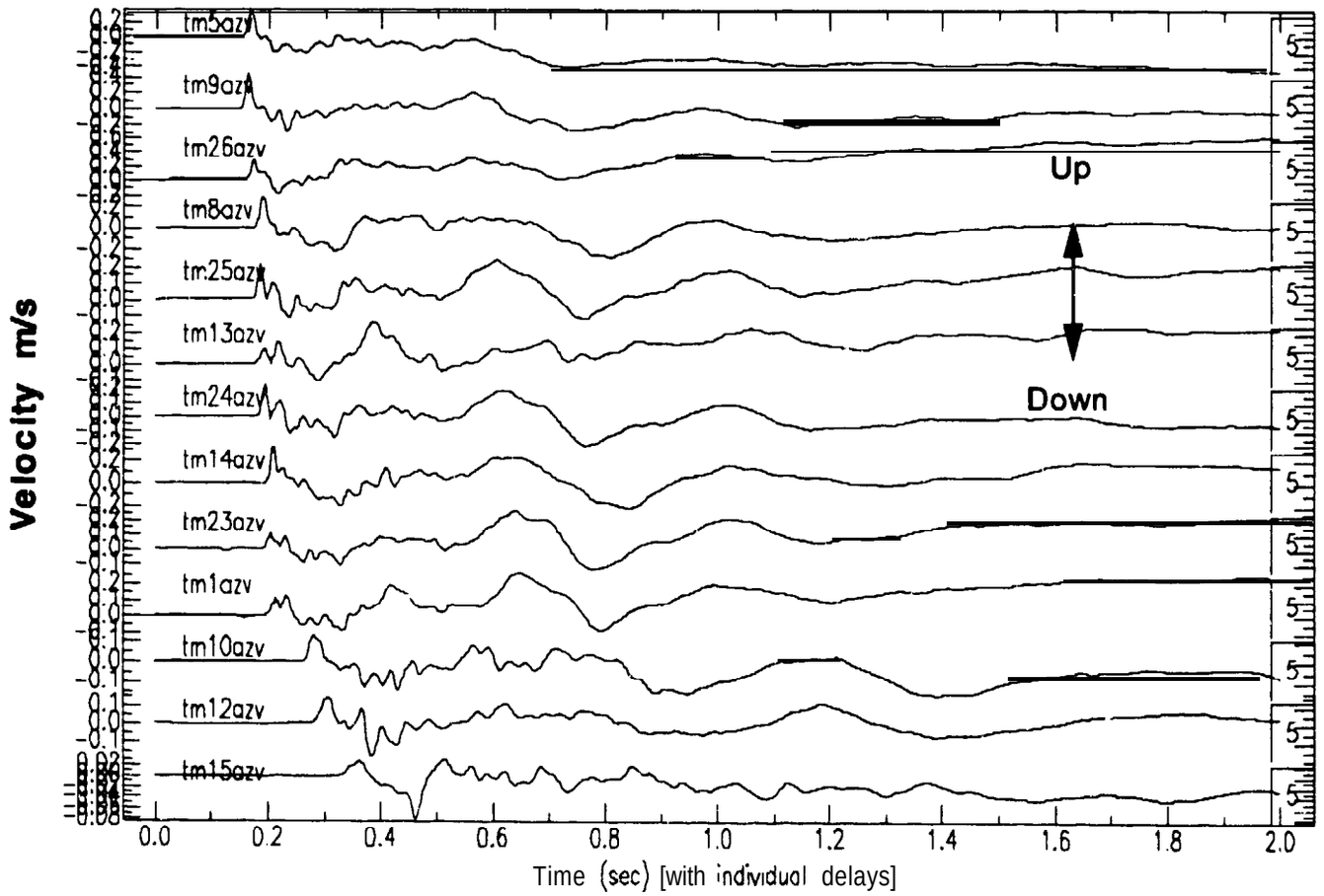

NPE - Station TM-10 (676 m)

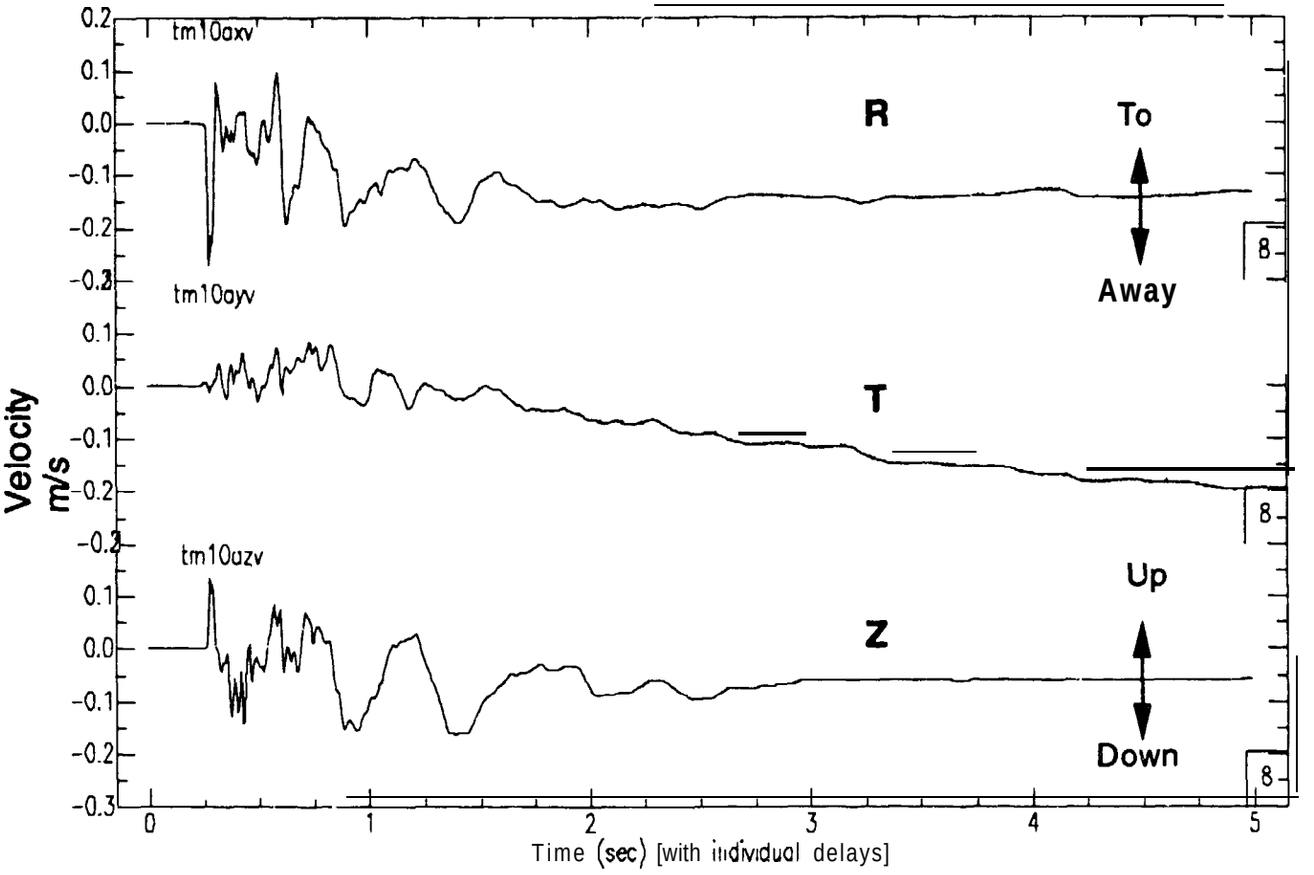

Fig. 4

MISTY ECHO Displacements - Radial

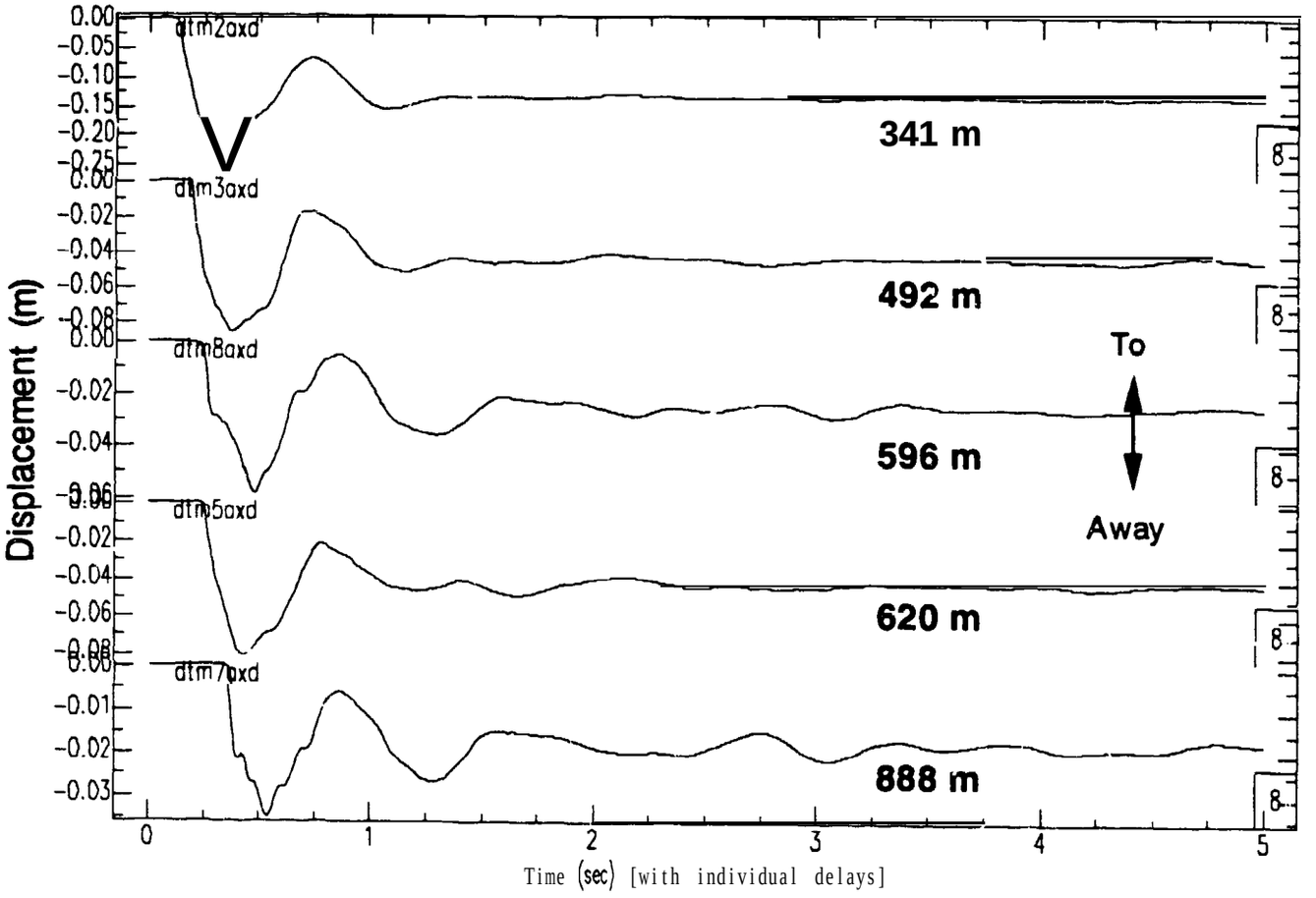

Fig. 5

MISTY ECHO - Radial Velocity waveforms

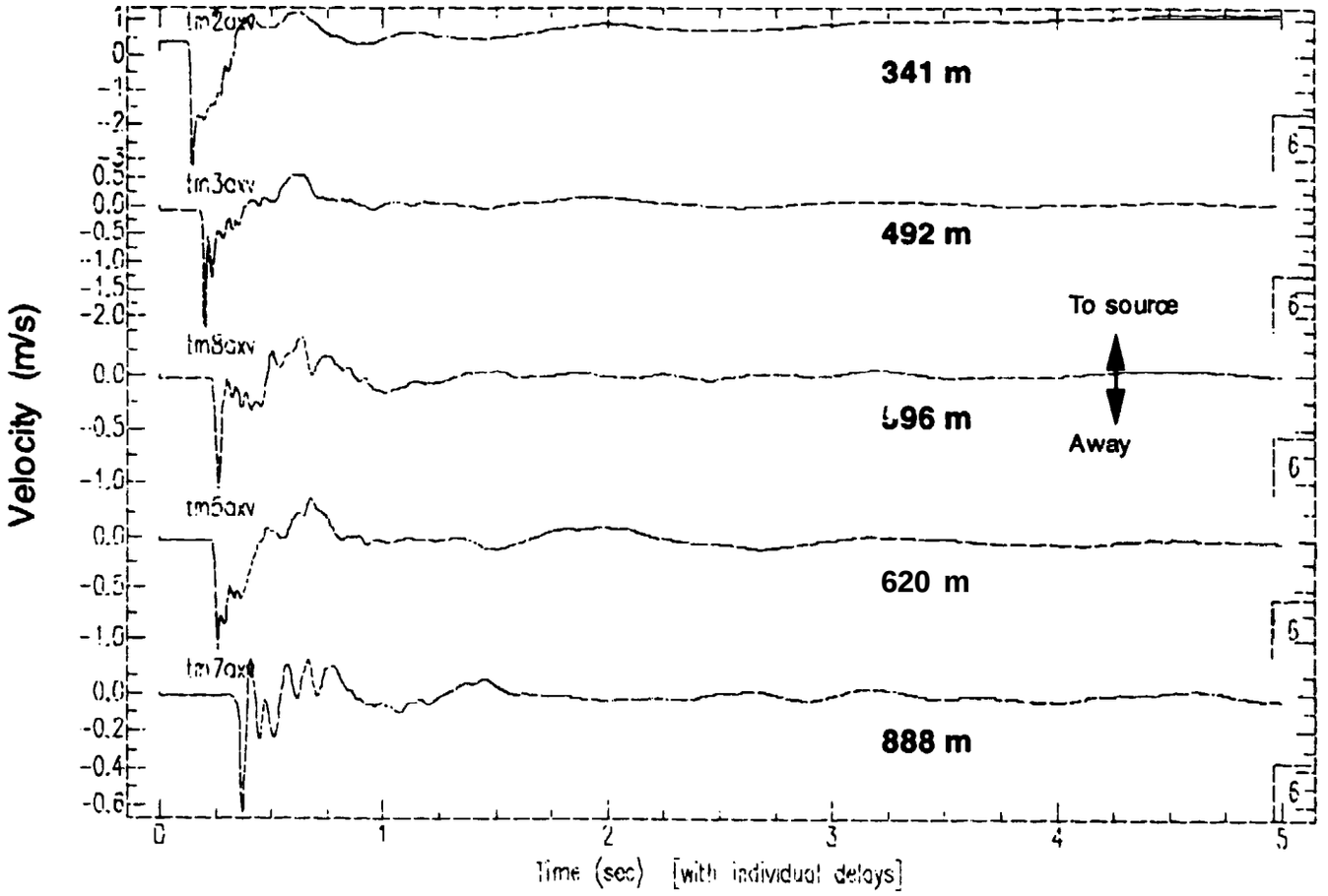

Fig. 6a

MISTY ECHO - Vertical (Z) Velocity waveforms

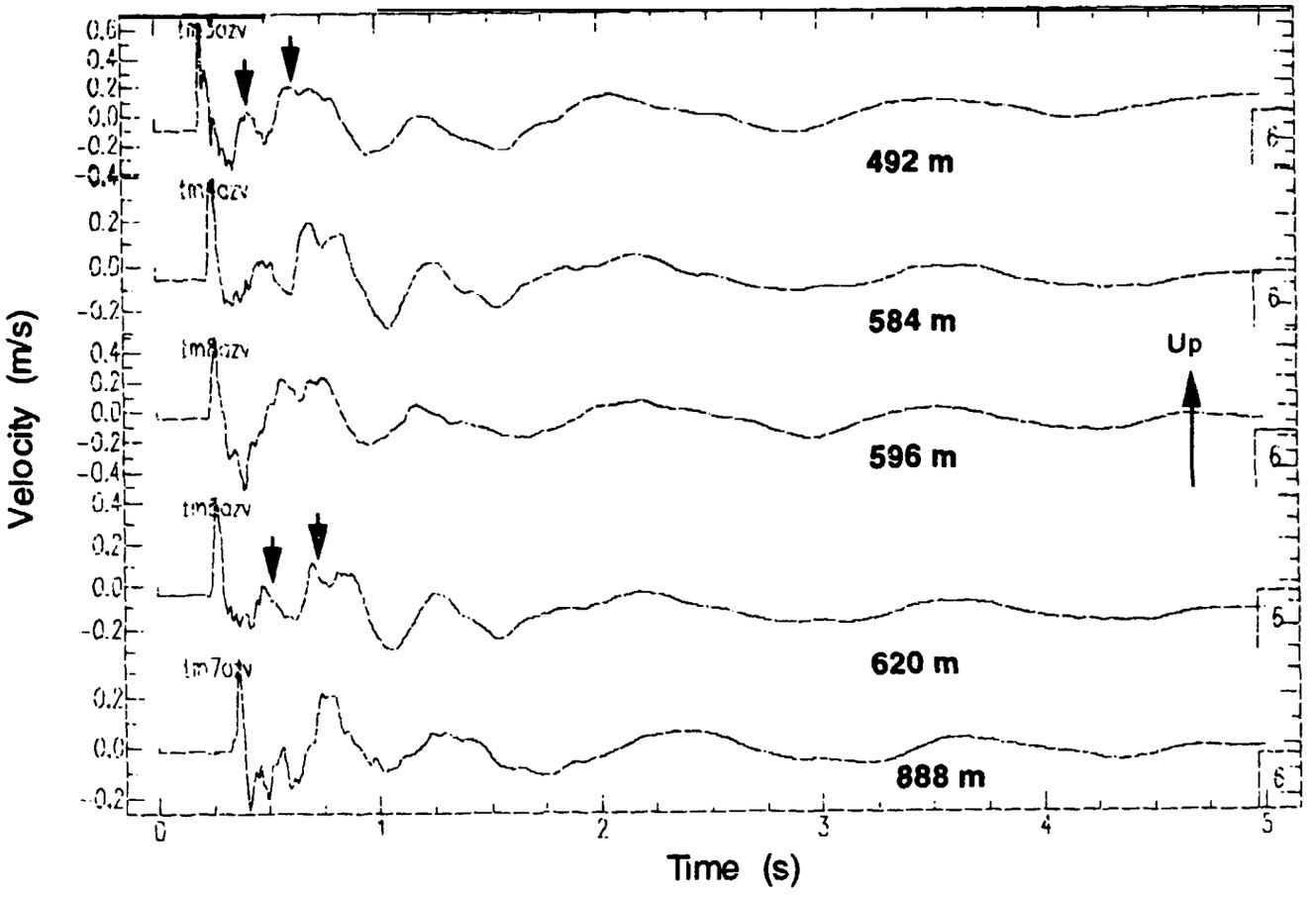

MISTY ECHO Velocities - Station TM-3 (492 m)

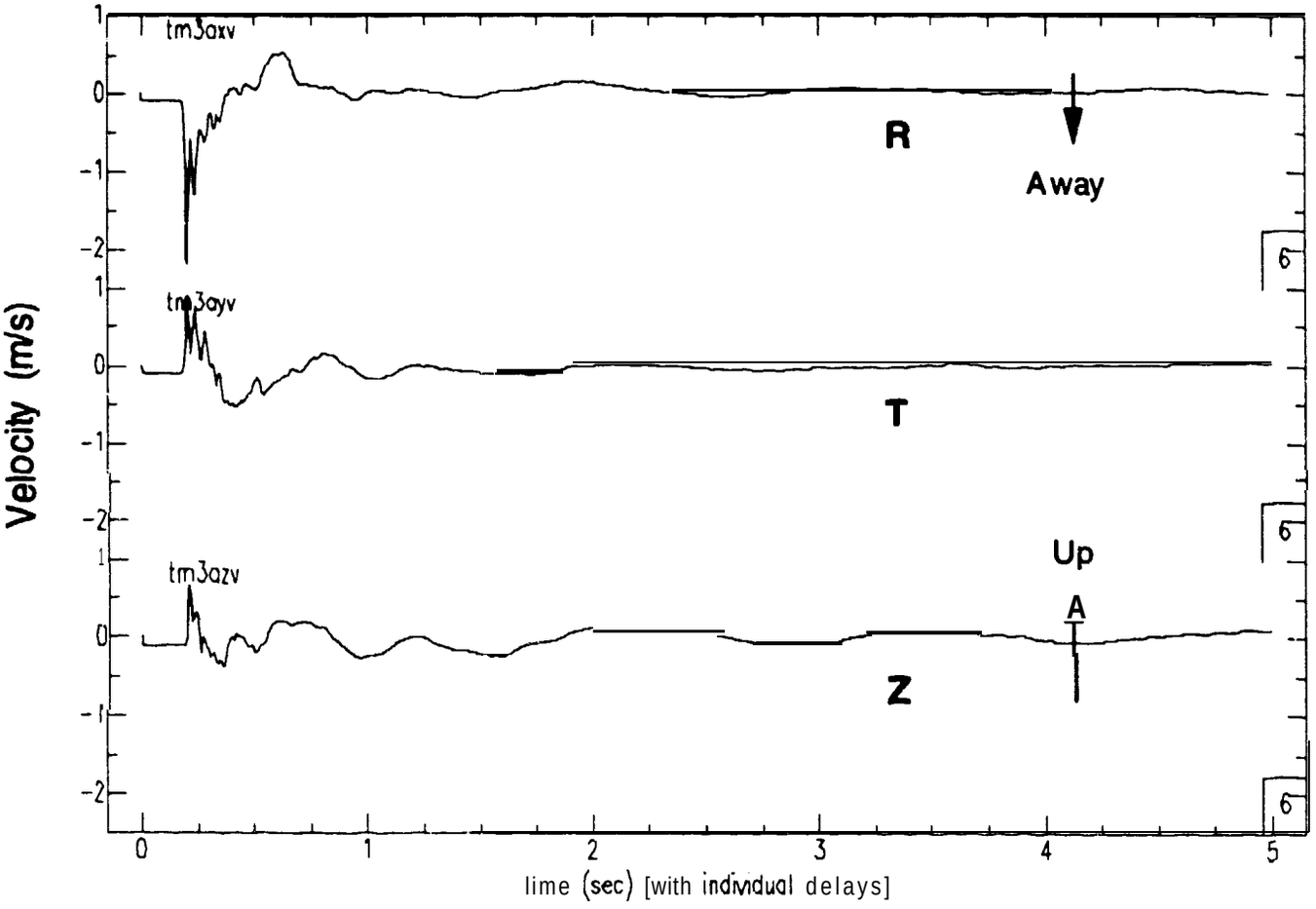

Fig. 7.